*Proceedings of the 21st ICSMGE, Vienna, Austria, 14 – 19 June 2026. Pistrol, Adam & Schweiger (eds.)*
*Published by: ÖGG, Austrian Society for Geomechanics, Salzburg, Austria, ISBN 978-3-9503898-4-5*
*https://doi.org/10.53243/ICSMGE2026-474*

# Geotechnical Centrifuge Modelling of Railway Embankments on Soft Clay Foundations

**Bas van Dijk**, Edo Vink
*Arcadis, The Netherlands, bas.vandijk@arcadis.com*

William Ovalle-Villamil
*Delft University of Technology, TU Delft, The Netherlands*

Cihan Cengiz
*Deltares, The Netherlands*

Agnes van Uitert
*ProRail, The Netherlands*

ABSTRACT: Many embankments of the Dutch railroad network are over a hundred years old and were constructed on very soft clay and peat layers. The weight of the trains and the use of the railway infrastructure have increased over time. A recent assessment of the stability of existing infrastructure revealed that the railway embankment is demonstrably not in compliance with the required standards in several locations. However, although considerable deformations exist in some cases, most of these embankments have remained stable under current use. This may indicate that several aspects of the train loading characteristics in relation to the foundation soil strength are not fully understood in the context of railway embankment stability. To better understand the effect of train loading and increased use of railroads on the soil strength, a geocentrifuge test program was executed through the GEOLAB initiative. During this study a series of centrifuge tests were performed of a railroad system composed of a sandy embankment underlain by a soft clay foundation, aiming to provide a better understanding of the potential effects of train loading characteristics and the increased use of railroads on the foundation soil strength. The models were tested in a geotechnical centrifuge at a gravitational acceleration field of 20g and included reference static monotonic tests to failure and tests modelling different train loading conditions, including different loading frequencies and amplitudes. This paper presents the design of the experimental setup, a description of the behavior's observed during the execution of the tests and preliminary results and observations of the project SURE performed as part of the transnational access initiative by GEOLAB. Further presentation and analysis of the results will be presented in a future companion article.

KEYWORDS: Railway embankment, soft clay, cyclic loading, centrifuge modelling.

## 1 INTRODUCTION

ProRail manages 7000 km of railway tracks built on approximately 3000 km of embankments. Many of these embankments were built on very soft clays and peats over 100 years ago, and the design did not consider the increased train loads and frequency of passages seen today (Van Uitert et al., 2023). With the anticipated further growth in railway infrastructure usage due to the need for sustainable transportation systems, there is a need for a better understanding of the behaviour and resilience of the Dutch embankments under both current and future loading scenarios. As such, ProRail launched the Embankment Programme in 2021 including the National Network Analysis of Embankments initiative (NNAE) that evaluates embankment stability using stochastic subsoil models derived from limited site-specific data. While the assessments often indicated failure to meet current standards for stability, the embankments appear to perform adequately under current use. Such a discrepancy highlights the need for specialised research on performance and modelling assumptions.

The project "Stability under increased Usage of Railway Embankments," or SURE, was carried out as a Transnational Access project within the GEOLAB framework to support this effort. SURE focused on the centrifuge modelling of a representative Dutch railway embankment founded on soft soils, replicating current and intensified traffic scenarios. The models allowed controlled testing of the embankment response under cyclic conditions with variable frequency and loading amplitude. This paper presents the model design used in SURE and preliminary results and observations. Although the study is ongoing, the insights from SURE contribute to a deeper understanding of embankment performance under intensified usage and offer a foundation for improving the assumptions and methodologies applied in large-scale assessment initiatives, such as the NNAE.

## 2 MODEL DESIGN

### 2.1 *Prototype Condition*

This study assessed a hypothetical 9-m-long section of a sandy embankment supporting a railway structure, with dimensions of 7 m in width, 1 m in height, and an underlying 6-m-thick soft clay foundation, as shown in Figure 1.

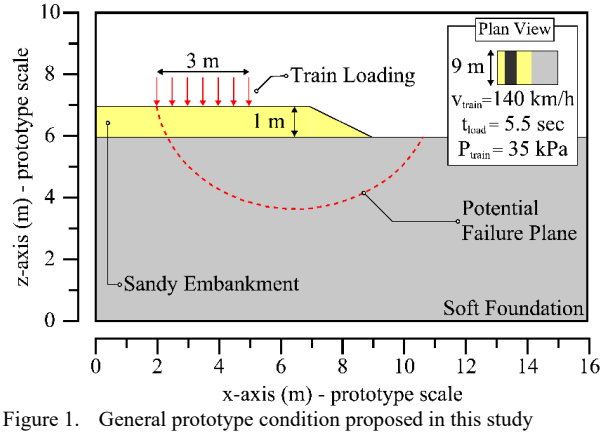


Figure 1. General prototype condition proposed in this study

The idealised loading conditions correspond to a Verlengd InterRegio Materieel (VIRM) train with eight coaches, each contributing to a design load of 35 kPa, as shown in Figure 2.

The total length of the train is 214 m, which traveling at a constant speed of 140 km/h results in a loading duration of nearly 5.5 seconds across the section studied. Each complete train passage was simplified as a single equivalent load to address the challenge of accurately replicating the intermittent loading from individual coaches in the centrifuge environment. Half-sine functions were employed to simulate train passage while preserving a realistic stress distribution and energy transfer to the embankment.


Figure 2. Idealized and simplified train loading conditions

Two intensity loading scenarios were evaluated: a) a train passing the control section every 10 minutes, which is a typical railway use in the Netherlands, and b) a train passing the control section every 4 minutes, resembling potential future use.

## 2.2 *Scaling Considerations*

Centrifuge modelling replicates stress conditions representative of full-scale geotechnical infrastructure by subjecting small-scale models to an increased gravitational field of N times Earth's gravity while using radial acceleration. Scaling laws of relevant physical variables are applied to ensure similarity between the model and prototype behaviour. This paper highlights relevant scaling laws in bold fonts for clarity. The fundamental relationships adopted follow classical centrifuge modelling principles (e.g., Goodings, 1982; Taylor, 1994; Iai et al., 2005; Garnier et al., 2007), where acceleration scales as $\mathbf{a}$ = N, lengths as $\mathbf{L}$ = N-1, and stresses as $\boldsymbol{\sigma}$ = 1, assuming identical materials in both model and prototype ($\boldsymbol{\rho}$ = 1).

The nature of the mechanisms modelled in this study required careful consideration of time scaling, as it involved kinematic and diffusion-driven processes. The duration of the train passage across the control section was interpreted as a kinematic event resulting from the train travelling at a constant speed between two fixed points, which can be scaled to the small-scale model with $\mathbf{v}$=1. This allows for the estimation of the loading duration atop the embankment through $\mathbf{t} = N^{-1}$. However, the generation and dissipation of excess pore pressures in the clay layers is a diffusion process for which adequate scaling laws indicate $\mathbf{v_{diff}} = N$ and $\mathbf{t_{diff}} = N^{-2}$. Since the embankment response was considered undrained during train loading, with strength development strongly linked to excess pore pressure generation and dissipation, the diffusion-based time scaling was adopted as the governing criterion for the experimental setup design.

## 2.3 *Experimental Setup and Small-scale Model Preparation*

The experimental setup shown in Figure 3a was designed for the 5.5 m-radius geotechnical centrifuge located at the University Gustave Eiffel, Nantes. This study used a centrifuge acceleration, or g-level, of 20g, based on the proposed prototype and scaling considerations, the anticipated failure plane, and the experimental capabilities available, including the dimensions of the strongbox and the maximum running time of 11 hours per test.

The setup included a rectangular steel strongbox with an integrated transparent wall, as shown in Figure 3b. The inner planar area was 80 cm by 45 cm, and its depth was 45 cm. A 30-cm-thick clay layer overlain by a 5 cm sand embankment was selected for the model geometry. An additional bottom sand layer underneath the clay allowed drainage during sample preparation. A 15-cm-width steel plate attached to a servo-controlled vertical actuator was used to model the train passages. The testing setup allowed continuous porewater pressure measurements at five locations within the foundation soil through a series of miniature pressure sensors, namely $PPT_1$ through $PPT_5$. The vertical displacement of the rigid plate was monitored through the displacement of the actuator, $d_A$, and two additional linear variable differential transformers (LVDT) placed on each side of the plate, $d_L$ and $d_R$. The increment in vertical load applied by the actuator to the embankment, $F_A$, was monitored through a load cell at the top of the rigid plate. Vertical deformations at different locations, $d_1$ through $d_4$, were also recorded using LVDTs. A video camera recording at variable frames per second through the transparent wall monitored the evolution of the tests.

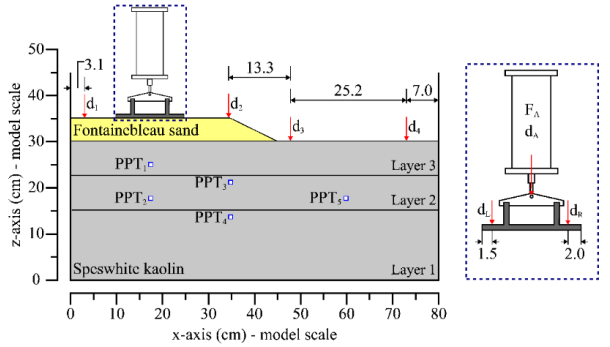


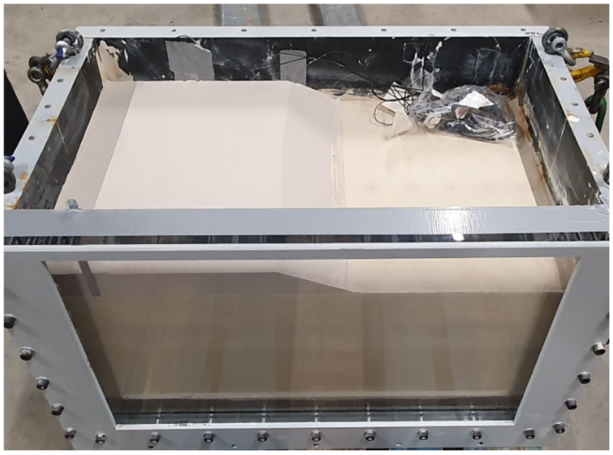

Figure 3. Experimental setup and model strongbox

The foundation soil used in this study was Speswhite kaolin clay (LL = 66, PI = 31, $G_s$ = 2.584), native from Germany. The foundation soil was prepared directly in the strongbox by consolidating three layers of clay slurry with an initial water content of 99% (i.e., 1.5 times LL). The initial void ratio, $e_i$, was estimated as 2.6. Each layer was consolidated with hydraulic (Test 1 and 2) and electrical (Test 3 and 4) presses using increments of surcharge load to a final pre-consolidation stress of 80 kPa (refer Section 2.4). After consolidation, the foundation soil's water content, $w_c$, void ratio, $e_0$, and saturated

unit weight, $\gamma_{sat}$, were approximately 44.7%, 1.18, and 17.2 kN/m$^3$, respectively.

After the foundation soil was prepared, a cover layer of uniform, fine-grained Fontainebleau sand ($d_{50}$ = 0.21 mm, $C_u$ = 1.47, $G_s$ = 2.65) native from France, was placed by dry pluviation to a final thickness of 5 cm and a dry unit weight of 16.3 kN/m$^3$ (e = 0.596, RD = 81%). The embankment was shaped afterwards by carefully removing the excess sand and trimming the slope to the final 2:1 (H:V) geometry.

### 2.4 *Pre-consolidation pressure*

To define the initial stress state and strength profile of the clay foundation in the centrifuge models, both laboratory data and numerical analyses were considered. Extensive laboratory testing performed on the clay material prior to the model preparation indicated SHANSEP parameters of S = 0.178 and m = 0.82, which allowed relating undrained shear strength to effective vertical stress and overconsolidation ratio.

To guide the selection of a representative pre-consolidation pressure for the model preparation, two-dimensional numerical analyses were carried out using finite element models in PLAXIS (Bentley Systems, 2023) and limit equilibrium models in D-Stability (Deltares, 2021). The train loading was modelled following the ProRail (2016) standard for a D4-type train, consisting of a 35 kPa distributed surface load over a 3 m width, combined with a 12.5 kPa ballast bed load. These models anticipated a failure plane approximately 2 m deep within the clay layer. The associated values of Factor of Safety for different assumed pre-consolidation pressures are presented in Figure 4.

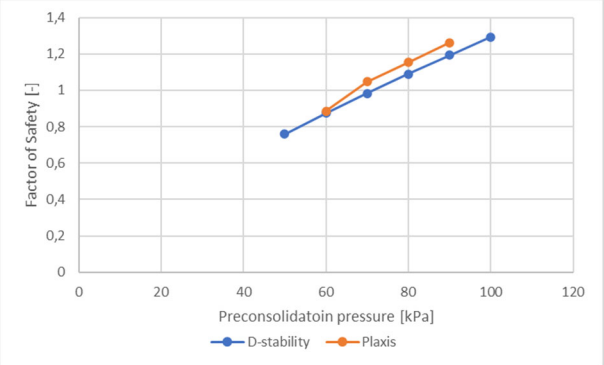


Figure 4. FoS at different pre-consolidation stresses

Based on these assessments, a pre-consolidation pressure of 80 kPa was selected for the model preparation. When combined with the SHANSEP framework, this pre-consolidation pressure led to an undrained shear strength profile ranging from approximately 11 kPa near the surface to 17 kPa at the base of the clay layer using a prototype scale.

### 2.5 *Experimental Protocol and Loading Conditions*

The experiments included three main stages. Stage 1 consisted of an initial consolidation phase, including maintaining a constant load $F_A$ = 473 N, equivalent to 7 kPa. Assuming another 5 kPa of ballast bed buried in the sand embankment of the model (to 0.7 m below the top of the track, refer to ProRail, 2016), this resembles a total ballast bed stress of 12 kPa. Stage 2 consisted of the cyclic loading of the embankment under various combinations of frequency and load amplitude resembling the prototype conditions proposed. Lastly, Stage 3 consisted of monotonic embankment loading until a maximum displacement of the loading plate of nearly 50 mm. Additional information obtained before, during, and after the experiments in selected models included surface plots, determination of pore pressure sensor locations after loading, Shear Vane Tests, water content measurements, and temperature evolution during flight.

Four tests were performed in this study. Tests 1 and 2 aimed to investigate the effects of the drainage conditions during monotonic loading. Test 1 used a drained loading of the embankment with a slow displacement rate, while Test 2 performed monotonic loading under fully undrained conditions. On the other hand, Tests 3 and 4 focused on the response of the embankment under various cyclic loading conditions to investigate the effect of increased usage of a railway due to an increase in train passages. Test 3 modelled the 10-minute passage condition, while Test 4 modelled a combined 10-minute and 4-minute passage condition. Figure 5 shows the shape of the cycles used to simulate train traffic in the cyclic loading tests.

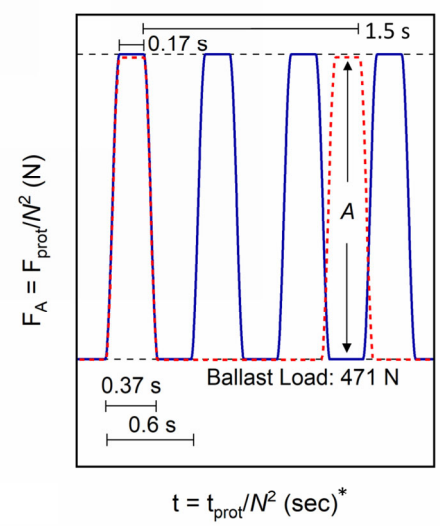


Figure 5. Scaled 10-minute (red) and 4-minute (blue) cycle. Only loading phase scaled as $\mathbf{t} = N^{-1}$

The duration of the loading phase, comprising the train arrival and departure from the section, was considered a kinematic condition scaled by $\mathbf{t} = N^{-1}$, resulting in a duration of 0.37 seconds, regardless of the total duration of the cycle. The total duration of the cycle, including train passing and wait time, was considered a diffusion event scaled by $\mathbf{t_{diff}} = N^{-2}$, resulting in total durations of 1.5 and 0.6 seconds for the 10- and 4-minute cases, respectively. It is also noted that the minimum load is constant and equivalent to the ballast load. Tests 3 and 4 included various combinations of load amplitude and a total number of cycles of 14,400 and 23,500, respectively.

It is worth noting that the response capability of the loading actuator was crucial for this kind of experiment. The loading duration in the proposed prototype condition is only six seconds, which resulted in scaled model times of a fraction of a second, as discussed above. This is sensitive to the g-level selected, and a larger g-level would decrease even further the required response time of the actuator. Under the conditions proposed, the load increase and decrease were modelled as a sinusoidal signal of 5 Hz with a plateau at the maximum load. The train passage was simulated under load-controlled conditions by the actuator to obtain the same load for each passage. Figure 6 shows a comparison of a random cycle from Test 3 with the design cycle, which highlights the quality of the experimental setup to reflect the prescribed load signal.

## 3 PRELIMINARY RESULTS

### 3.1 *Soil Investigation*

Each test included three to four in-flight Cone Penetration Tests (CPT) at various locations within the models, including the far field side, near the toe of the embankment, and at the crest. The CPT tests were performed after the consolidation stage and again after the monotonic loading phase. For the latter tests, the centrifuge was briefly stopped to allow repositioning of the cone.

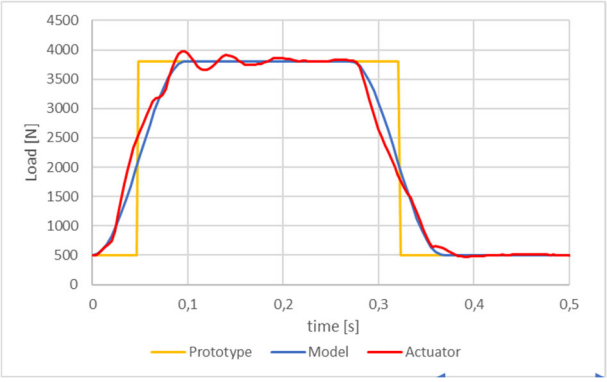


Figure 6. Prototype, model and actuator load.

Additional Vane Shear Tests were also performed approximately one day after the end of each experiment and under 1g conditions. The tests used a four-blade vane with a length of 50 mm and a width of 33 mm. Other element tests carried out from samples recovered at the end of each experiment included, among others, consolidated undrained triaxial tests (under a confining stress of 40 kPa), direct shear tests (under a vertical stress of 40 kPa), and direct simple shear tests (under vertical stresses of 20, 40, and 80 kPa).

Figure 7 shows the results from CPT, Vane Shear, and element tests obtained across all models. For the CPTs, an $N_k$ factor of 13.5 was used to correlate the cone resistance, $q_c$, with the undrained shear strength, $S_u$, which nicely matched the measured cone resistance to the measured undrained shear strength of the vane and laboratory tests. The estimated values of $S_u$ varied between 12 and 18 kPa and slightly increased with depth. Values of $S_u$ above 0 m correspond to penetration into the embankment and are not representative of the clay. The observed strength profile aligns reasonably well with the predicted trend based on the SHANSEP parameters, as shown in see Figure 8.

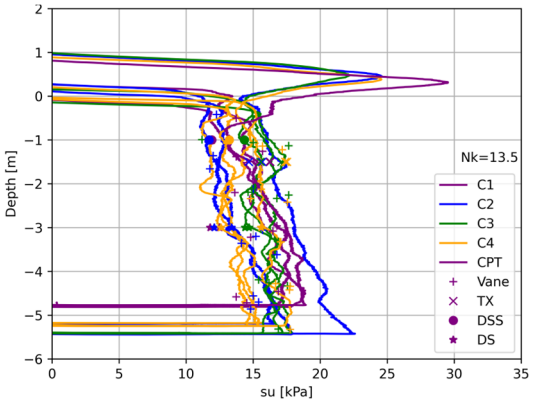


Figure 7. Measured undrained shear strength.

A potential concern during the experimental program was the possible dehydration of the sample surface during the prolonged centrifuge runs of up to 11 hours. In the first two tests, this was mitigated by covering the sample surface with plastic foil. For the last two tests, this measure was omitted. However, water content measurements taken at the end of the centrifuge tests and alongside the element testing samples showed relatively similar values and not significant dehydration, except for one outlier likely due to measurement error, as shown in Figure 9. Overall, measured water contents ranged between 40% and 50%, supporting the consistency and reliability of the strength parameters obtained from post-test element testing.

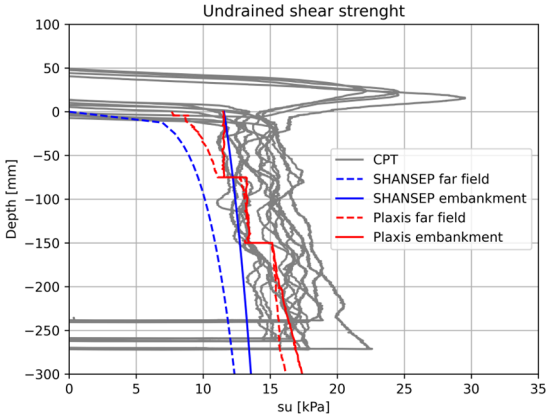


Figure 8. Predicted versus measured undrained shear strength.

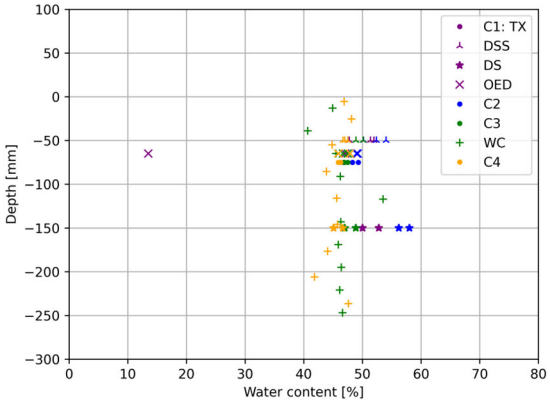


Figure 9. Water content measurements.

### 3.2 *Monotonic Loading Sequences*

Figure 10 shows the evolution of the vertical stress induced, $\sigma_v$, and the pore-pressure at $PPT_2$, as functions of the actuator displacement, $d_A$, obtained during the monotonic loading sequences. Tests 1 and 2 showed very similar behaviours while loading to failure despite the conceptual differences proposed for each test. After a three-hour consolidation period in Test 1, the magnitude of $F_A$ was increased under low actuator displacement rates. The loading continued with the expectation of inducing a drained condition until failure. However, while the load slowly increased, also the porewater pressure increased, indication undrained loading. Consequently, the displacement rate was decreased in several occasions during this test so that the porewater pressures could dissipate. Despite the efforts, the pore pressure sensors indicated pressure buildup during loading, and undrained or partially drained behaviour was likely reproduced. In contrast, Test 2 was performed under the largest displacement rate possible and after nearly eight hours of consolidation. Tests 3 and 4 display a larger initial stiffness, compared to Tests 1 and 2, describing hardening behaviour resulting from the cyclic loading. The results from Tests 1 and 2 did not show a distinct peak in the magnitude of $\sigma_v$ during monotonic loading. Instead, it continued increasing

beyond large displacements of up to 1 m in the prototype scale. As a result, a representative ultimate resistance could not be clearly defined. In contrast after cycling, Test 3 and 4 showed an increase in stiffness and a much more pronounced failure peak.

### 3.3 *Cyclic Loading Amplitude*

Determining an adequate cyclic loading amplitude for Tests 3 and 4 required balancing the competing goals of inducing a meaningful plastic deformation without triggering a failure mechanism prematurely (i.e. prior to the monotonic loading sequence) and studying load amplitudes representative of historical use. Although a typical target amplitude could be a factor of nearly 1.2 times lower than the ultimate resistance,

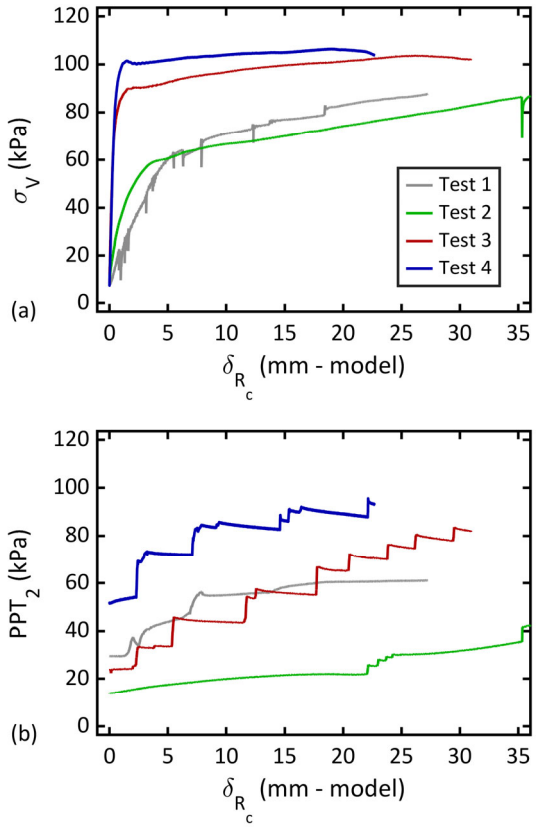


Figure 10. Vertical stress and pore pressure during monotonic loading

As an alternative, Tests 3 and 4 followed an initially low cyclic loading amplitude with short, stepped increments after 100 cycles until reaching the load at which plastic deformation occurred in the monotonic loading tests. For a fair comparison between the cyclic tests, the same load amplitudes and number of cycles were reproduced in both Tests 3 and 4 for the initial 5,400 cycles. Afterwards, the frequency of loading changed following the prototype scenarios considered in this study. Neither Test 3 nor 4 failed before the monotonic loading phase.

### 3.4 *Image analysis and deformation mechanism*

Visual recordings were obtained throughout the experiments to analyse the various events reproduced. The characteristic light colour and low contrast of the foundation clay posed a challenge for image analysis in the absence of artificial seeding, which was particularly evident during Tests 1 and 2, as shown in Figure 11. To improve contrast in later tests, horizontal lines of dark-coloured sand were embedded between layers during sample preparation for Tests 3 and 4. Despite these imaging challenges, particle image velocimetry (PIV) analysis using PIVlab (Thielicke and Sonntag, 2021), combined with the PIV-NP approach (Pinyol and Alvarado, 2017), enabled the identification of shear band development within the embankment and clayey soils, as well as the deformation and evolution of failure planes across different stages of loading. Preliminary results of this analysis are presented in Figures 12 and 13, showing the shear strain fields for selected stages during monotonic loading (see Figure 10). While ongoing work aims to refine the analysis, the current results provide valuable insight into the deformation mechanisms captured in the model.

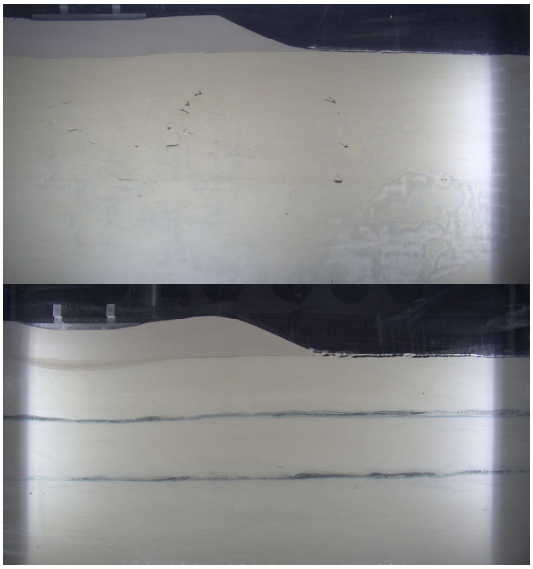

Figure 11. Example of model frames from (a) Test 2 and (b) Test 4. Frames taken at estimated yield stress

## 4 CONCLUSIONS

To improve the understanding of the potential effects of train loading and increased use of railroad systems built on soft soils, a geotechnical centrifuge testing program was executed through the GEOLAB initiative. A series of centrifuge tests was performed using railroad models composed of a sandy embankment underlain by a soft clay foundation, resembling a typical context for Dutch infrastructure.

The study integrated extensive element testing before and after the experimental campaign to support both model design and the interpretation of results. Likewise, numerical assessments using different methodologies served as input for estimating relevant parameters, such as pre-consolidation pressure and undrained shear strength. The in-situ and postmortem element tests matched reasonably well with the intended shear strength profile.

The g-level was carefully selected, considering the box dimensions, the expected slip circle dimensions, the capabilities of the actuator to perform the loading cycles and the dissipation time between load cycles. During the tests, the actuator performed well delivering over ten-thousand load cycles, nicely matching the intended load cycles during many hours of centrifuge testing.

It was attempted to perform a drained load test. Even though the load test lasted for a few hours, the pore pressure sensors still indicated excess pore pressure build up.

Although the Speswhite clay has a low contrast posing a challenge for image analysis, the PIV-NP approach enabled the identification of shear band development and the evolution of failure planes.

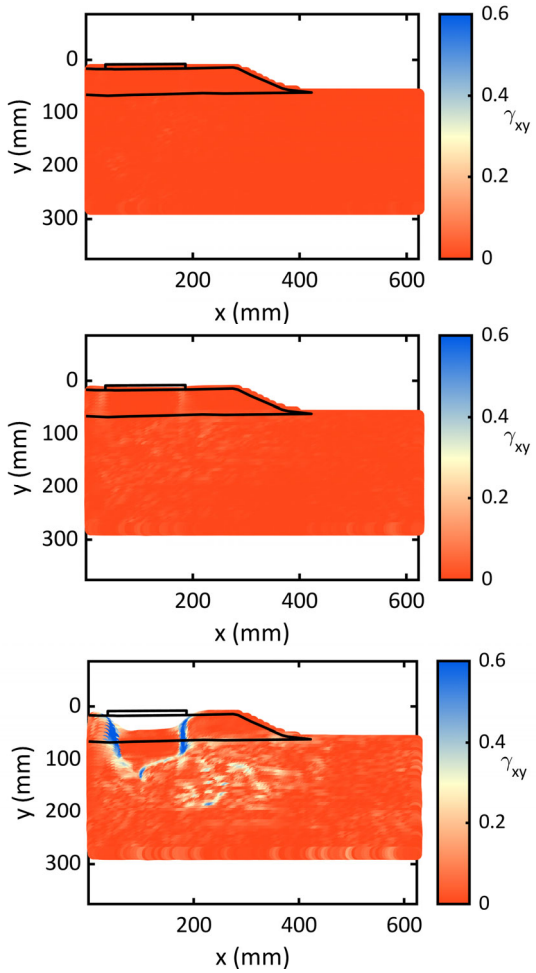


Figure 12. Estimation of shear strain during monotonic loading stage in Test 2: (a) initial conditions, (b) at estimated yield stress, and (c) after a large displacement. Deformations extending beyond the original surface tracking area are not shown, although they did occur during the test.

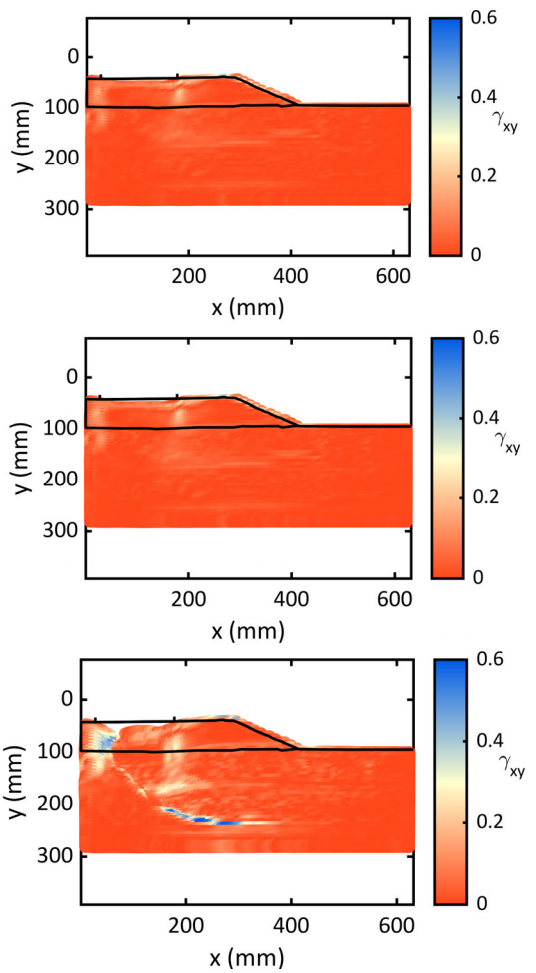


Figure 13. Estimation of shear strain during monotonic loading stage in Test 4: (a) at end of cyclic loading, (b) at estimated yield stress, and (c) after a large displacement. Deformations extending beyond the original surface tracking area are not shown, although they did occur during the test.

The outcomes of this study contribute to a deeper understanding of embankment performance under intensified loading and may serve as a valuable reference for the refinement of numerical models used in the assessment of railway infrastructure on soft soils. However, at the time of writing, the evaluation of the results is still ongoing. In a companion article the results of the centrifuge tests, together with an evaluation and discussion, will be presented in more detail.

## 5 ACKNOWLEDGEMENTS

The work was funded by the European Union's Horizon 2020 GEOLAB project (Grant No. 101006512). The authors gratefully acknowledge the GEOLAB community, the Université Gustave Eiffel Nantes, ProRail, Deltares, TU Delft and Arcadis for their support to this article and for improving geotechnical practice.

## 6 REFERENCES

Bentley Systems. 2023. *PLAXIS 2D Reference Manual*. Bentley Systems, Inc., Delft, The Netherlands.

Deltares. 2021. D-Stability 2021 [Computer Software]. https://download.deltares.nl/d-stability

Garnier, J., Gaudin, C., Springman, S. M., et al. 2007. Catalogue of scaling laws and similitude questions in geotechnical centrifuge modelling. *International Journal of Physical Modelling in Geotechnics*, 7(3), 1.

Goodings, D.J. 1982. Relationships for centrifugal modelling of seepage and surface. *Géotechnique*, 32(2), 149-152.

Iai, S., Tobita, T., and Nakahara, T. 2005. Generalised scaling relations for dynamic centrifuge tests. *Géotechnique*, 55(5), 355-362.

ProRail, 2016. *Richtlijn Beoordelen constructieve veiligheid bestaande Baanlichamen* , RLN00414-1

Pinyol, N.M. and Alvarado, M. 2017. Novel analysis for large strains based on particle image velocimetry. *Canadian Geotechnical Journal*, 54(7), pp.933-944.

Taylor, R. N. 1994. *Geotechnical Centrifuge Technology*, 1st Ed, CRC Press.

Thielicke W. and Sonntag, R. 2021. Particle Image Velocimetry for MATLAB: Accuracy and Enhanced Algorithms in PIVlab. *Journal of Open Research Software*, 9(1), Ubiquity Press, Ltd.

Van Uitert, A., Van Eeten, S., Verbruggen, D., 2023. The Geotechnical state of the railway embankments in The Netherlands / De Geotechnische staat van de spoorbaan in Nederland, *ISSMGE Geotechniekdag2023-4*